Supplementary Figure 1a-e

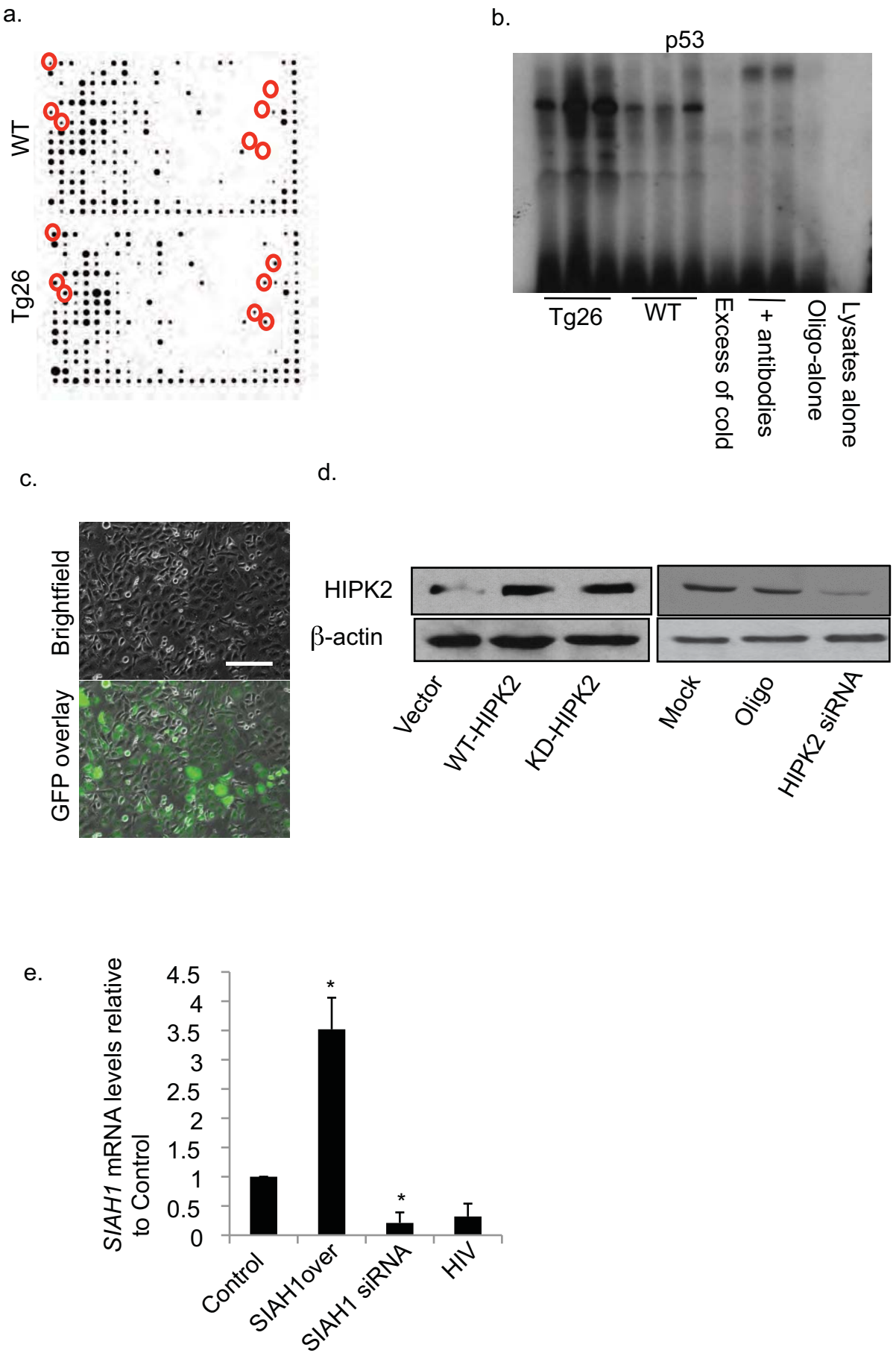

Supplementary Figure 1: Validation of protein/DNA interactions in wild-type (WT) and HIV transgenic (Tg26) kidneys and renal tubular cell transfection efficiency. (a) Affymatrix/Panomics protein/DNA arrays for a wildtype (WT) and a HIV transgenic (Tg26) kidney. Spots that are significantly different are outlined in red. Differentially regulated transcription factors are listed in Supplementary Table b. (**b)** Electrophoretic mobility shift assay (EMSA) was used to confirm the regulation of these transcription factors. An example of EMSA is shown for p53. (**c**) Transfection efficiency of human renal tubular epithelial cells (hRTECs) using Lonza's Nucleofector Technology was verified using a GFP-HIPK2 fusion construct. Scale bar, 20μm. (**d**) Over-expression of wild-type (WT)- and kinase-dead (KD)- HIPK2 constructs, and knock down of HIPK2 by siRNA (HIPK2 siRNA) in hRTECs were confirmed by Western blotting. Vector: empty expression vector. Mock: transfection without siRNA oligonucleotide. Oligo: negative control siRNA. (**e**) SIAH1 expression as quantified by real time PCR in hRTECs transfected with an empty expression vector (Control), a SIAH1 expression construct (SIAH1over), a siRNA against SIAH1 (SIAH1 siRNA), or the pNL4-3 HIV-1 construct (HIV). *$p<0.05$ compared to Control. n=3 for each group. SIAH1 siRNA also reduced protein expression of SIAH1 (Fig 3f).

Supplementary Figure 2a-c

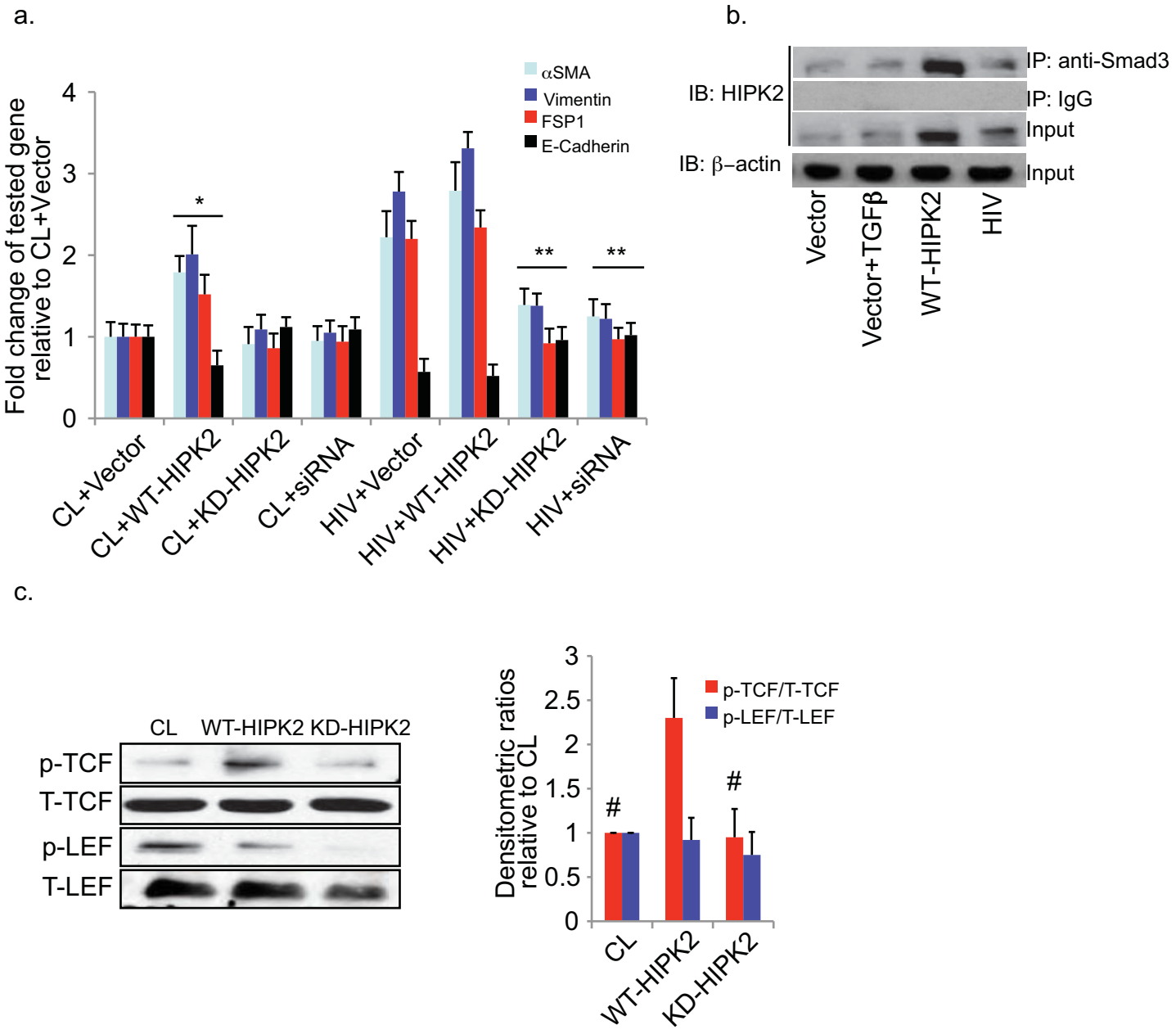

Supplementary Figure 2d-e

d.

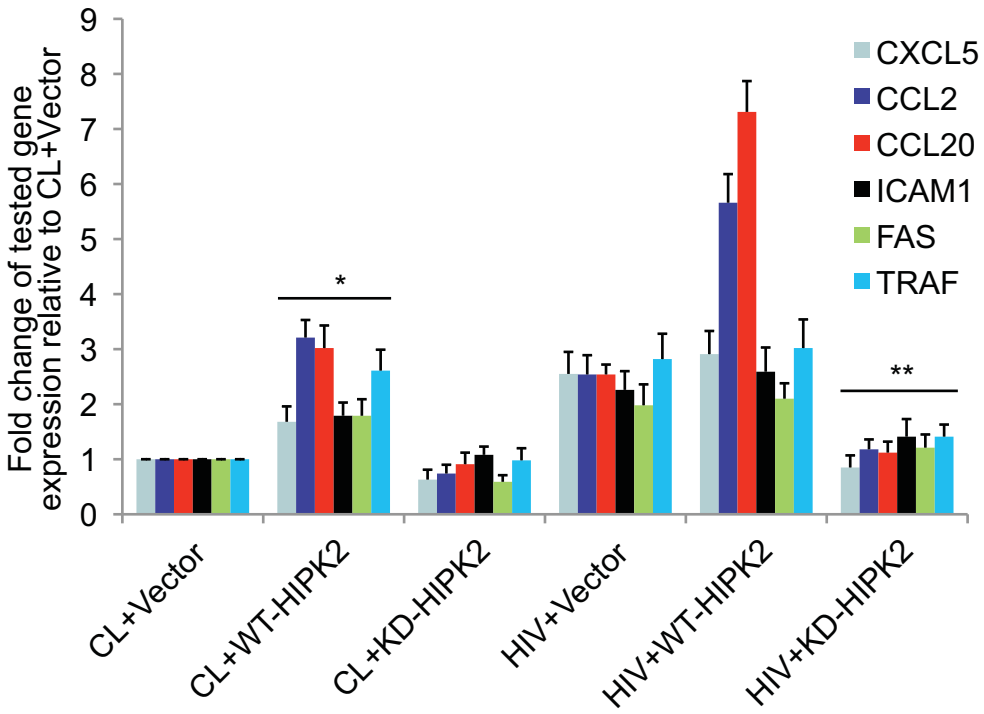

e.

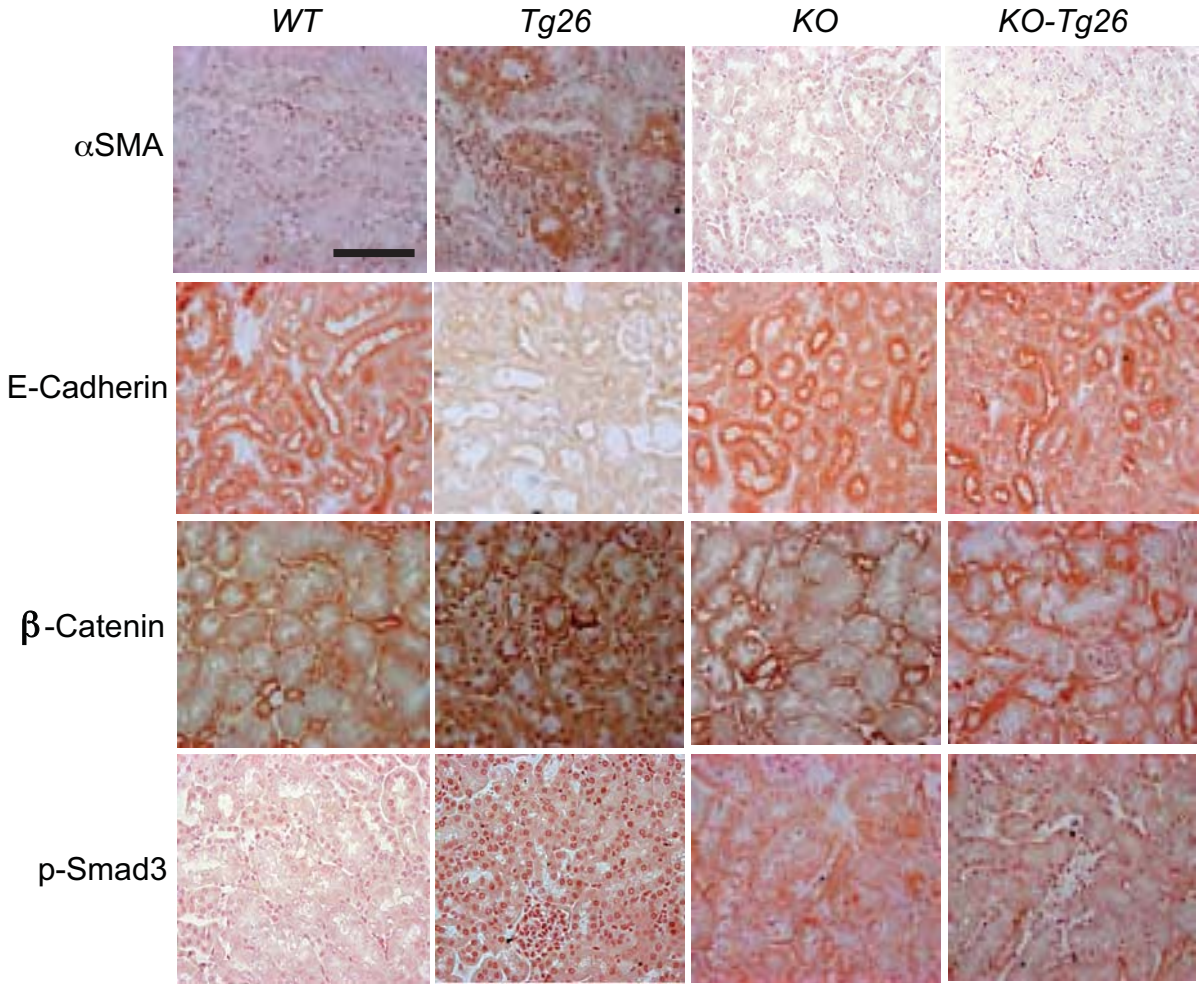

Supplementary Figure 2: HIV promotes the expression of markers of epithelial mesenchymal transition, NFkB signaling, Smad3 binding to HIPK2, and phosphorylation of transcriptional regulators of Wnt signaling in renal cells. (**a**) Real-time PCR quantification of EMT markers in HK2 cells infected with a control (CL) or HIV pseudotyped virus (HIV) and transfected with an empty expression vector (Vector), a wild-type HIPK2 (WT-HIPK2) expression vector, a kinase dead HIPK2 (KD-HIPK2) expression vector, or a HIPK2 siRNA (siRNA). n=4. (**b**) Co-immunoprecipitation of HIPK2 and Smad3 in nuclear lysate of HK2 cells transfected with Vector with and without TGFβ (5 ng/ml) treatment, transfected with WT-HIPK2, or infected with HIV. Immunoprecipitation (IP) was carried out with either an anti-Smad3 antibody or normal rabbit IgG (IgG) as control. Immunoblotting (IB) was performed using an antibody to HIPK2 and β-actin. Input = nuclear lysate prior to IP. Western blots (**c. left panel**) and densitometric ratios (**c. right panel**) of phospho and total TCF and LEF in nuclear lysates of hRTECs transfected with CL, WT-HIPK2 or KD-HIPK2. #$p<0.05$ compared to WT-HIPK2 for p-TCF/T-TCF only, n=3. (**d**) Expression of NFkB target genes in primary hRTECs infected with HIV or CL virus and transfected with Vector, WT-HIPK2 or KD-HIPK2. n=4. *$p<0.05$ compared to CL+Vector for each of the tested genes. **$p<0.05$ compared to HIV+Vector for each of the tested genes. (**e**) Immunostaining of αSMA, E-Cadherin, β-Catenin and p-Smad3 in kidney sections of WT, Tg26, KO, and KO-Tg26 mice. Representative pictures of 5 mice in each group are shown. Scale bar, 100μm.

Supplementary Figure 3a-f

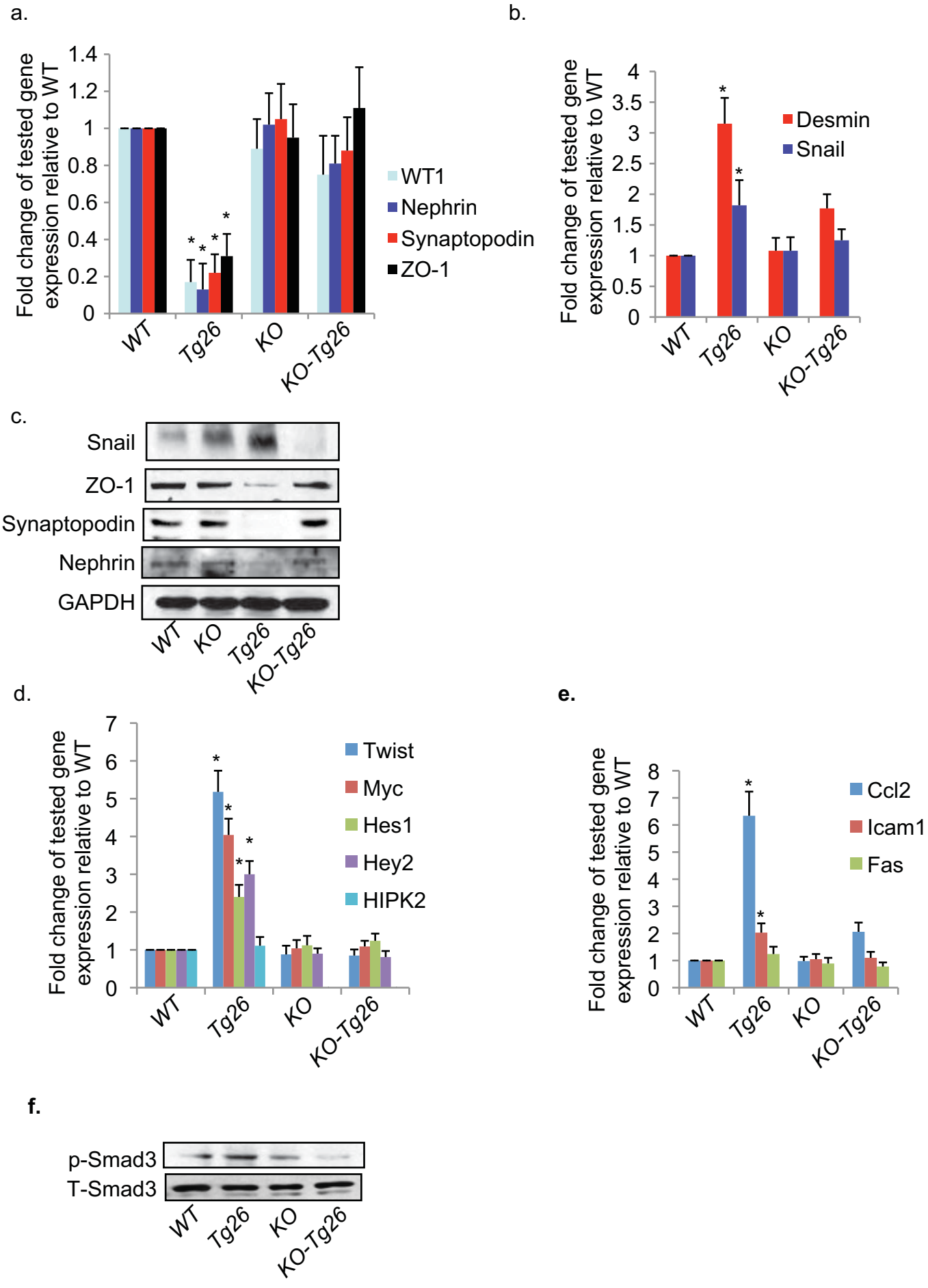

Supplementary Figure 3g-j

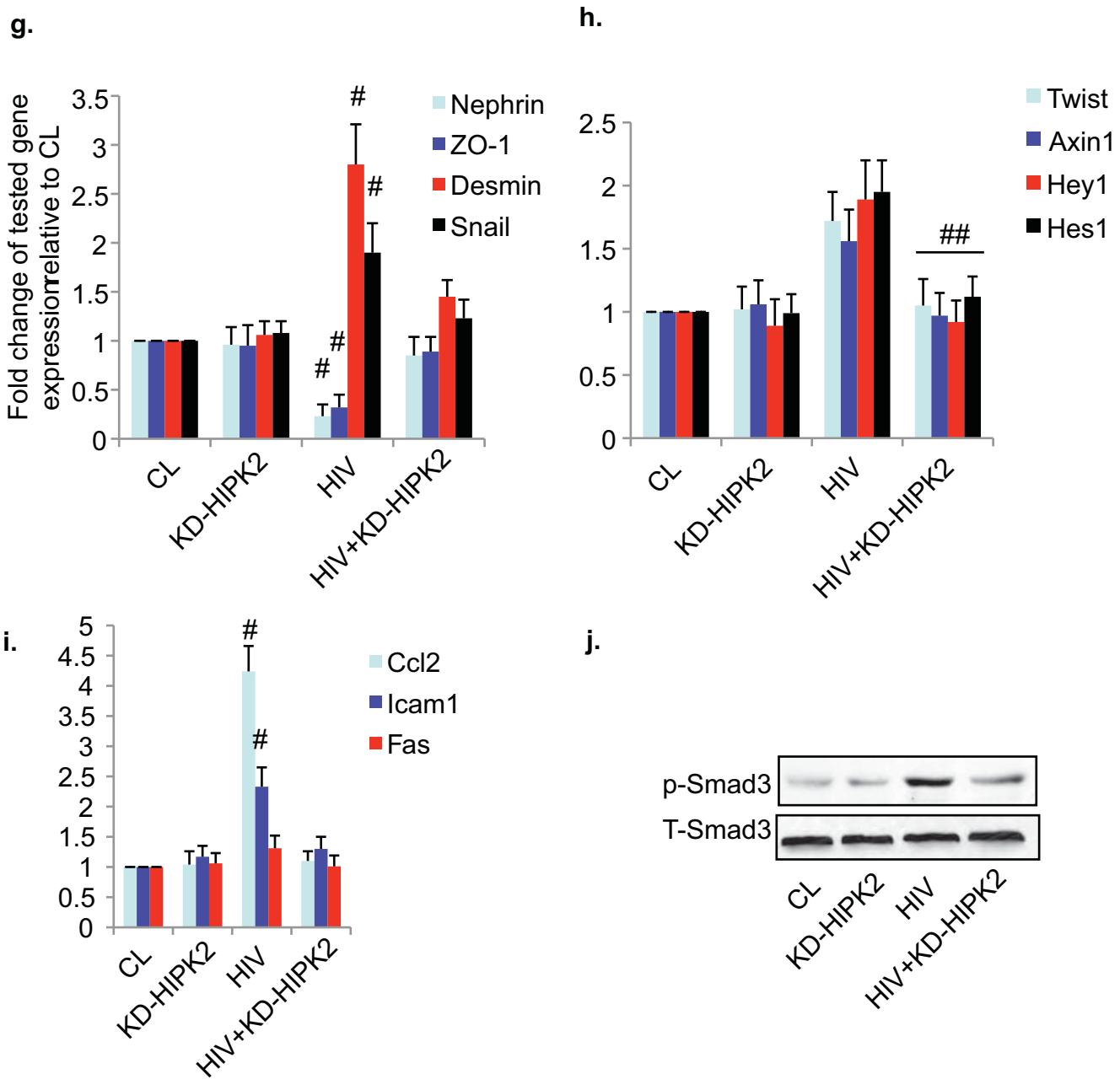

Supplementary Figure 3: HIKP2 knockout (KO) in Tg26 mice attenuates loss of podocyte differentiation markers and increased in mesenchymal markers and Wnt/Notch and NFkB target gene expression. Expression of markers of differentiated podocytes (**a**) and epithelial mesenchymal transition (**b)** in glomeruli isolated from wild-type (WT) and Tg26 mice with and without HIPK2 knockout (KO) at age of 8 weeks. (**c**) Western blots of Snail, ZO-1, synaptopodin, nephrin, and GAPDH in isolated glomeruli. Glomerular expression of target genes of Wnt/Notch (**d**) and NFkB (**e**) signaling. (**f**) Western blots of phospho- and total- Smad3 (p- and T-Smad3) of isolated glomeruli. Expression of podocytes differentiation markers (**g**) and of Wnt/Notch (**h**) and NFkB (**i**) signaling in differentiation conditionally immortalized murine podocytes infected with the pNL4-3 pseudotyped virus (HIV) or a control virus (CL) and transfected with a control vector or a kinase dead HIPK2 (KD-HIPK2) expression construct. (**j**) Western blots of p-Smad3 and T-Smad3 in nuclear lysates. *$p<0.05$ compared to corresponding gene in the WT group. #$p<0.05$ compared to corresponding gene in the CL group. ##$p<0.05$ compared to the HIV group. n = 4 for each group. WT1 = Wilms Tumor 1. ZO-1 = tight junction protein ZO-1.

Supplementary Figure 4a-d

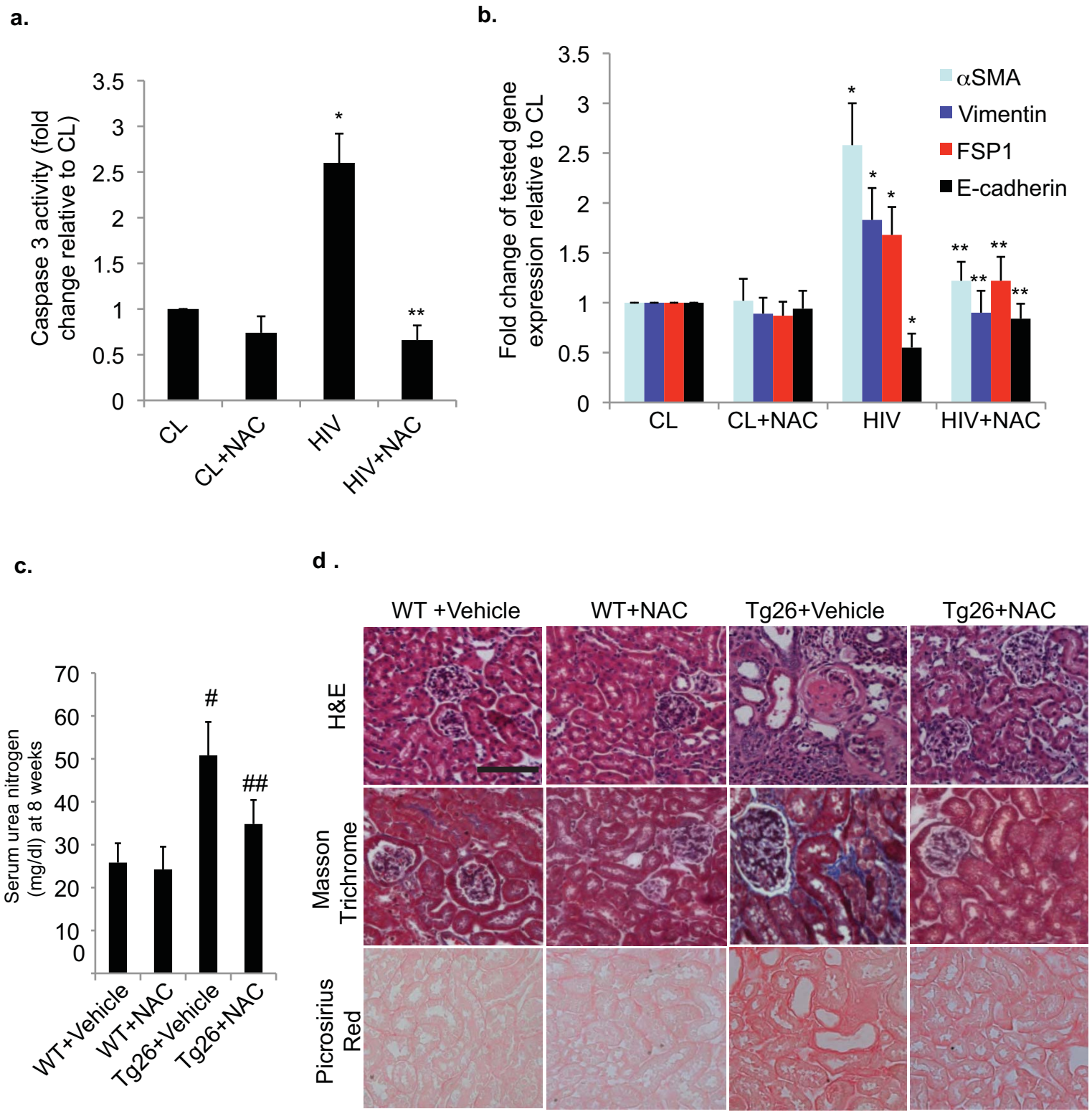

Supplementary Figure 4e-h

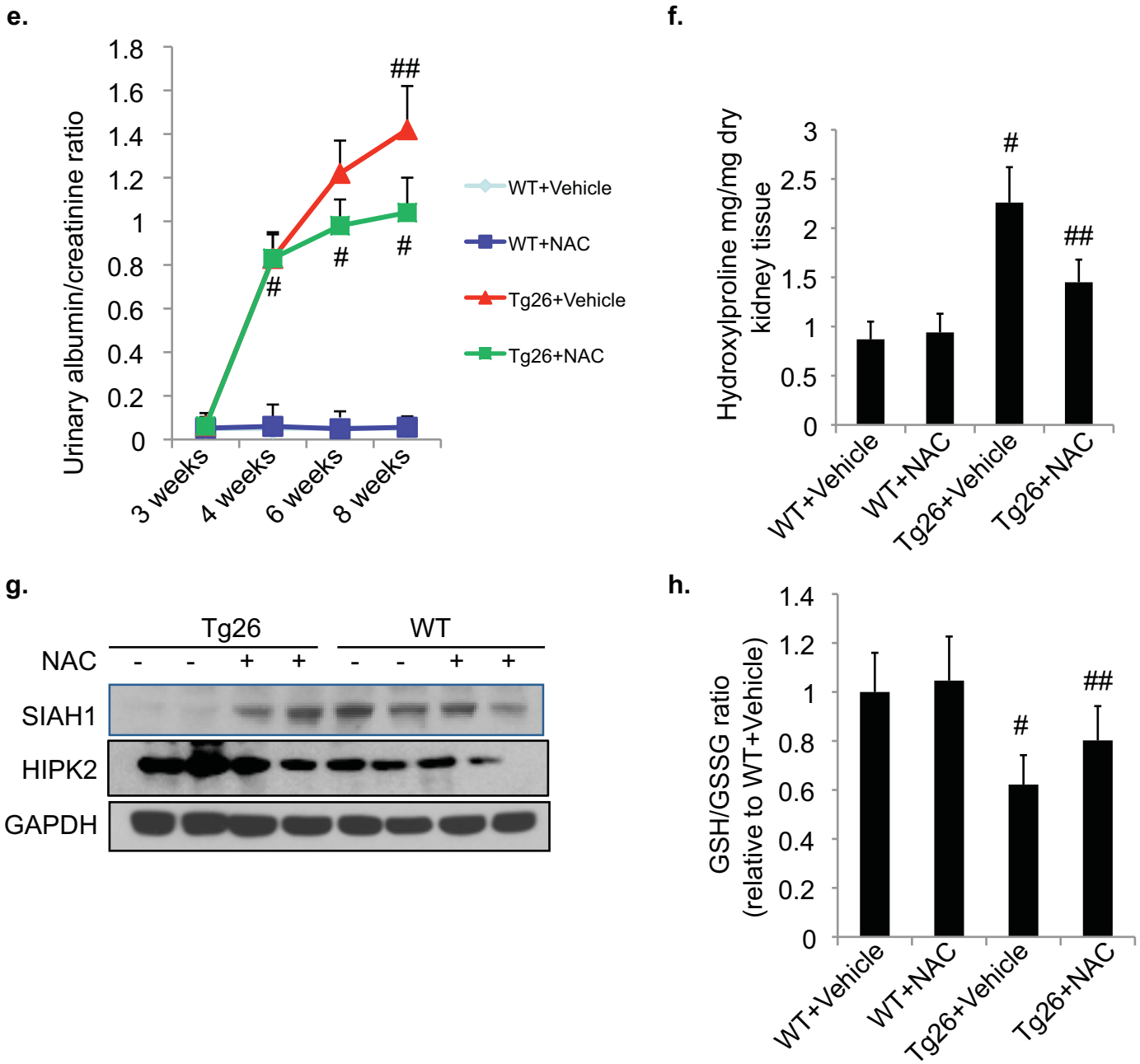

Supplementary Figure 4: N-Acetyl-cysteine (NAC) treatment abrogates renal fibrosis in Tg26 mice by suppressing HIPK2 expression. Activity of caspase 3 (**a**) and expression of epithelial mesenchymal transition markers (**b**) in hRTECs infected with HIV pseudotyped virus (HIV) or control virus (CL) and treated with or without N-acetylcysteine (NAC, 10mM). Serum urea nitrogen (**c**), renal histology (**d**), urine albumin to creatinine ratio (**e**), kidney hydroxyproline content (**f**), Western blots of SIAH1 and HIPK2 (**g**), and tissue ratio of reduced to oxidized glutathione (GSH/GSSH, **h**) in Tg26 and WT mice treated with either vehicle or NAC from age of 4 to 8 weeks by daily gavage as described in the Methods. *p< 0.01 compared to CL. **p< 0.01 compared to HIV, n=4. #p<0.01 compared to WT+Vehicle. ## p< 0.05 compared to Tg26+vehicle, n=10. Scale bar, 100μm.

Supplementary Figure 5a-c

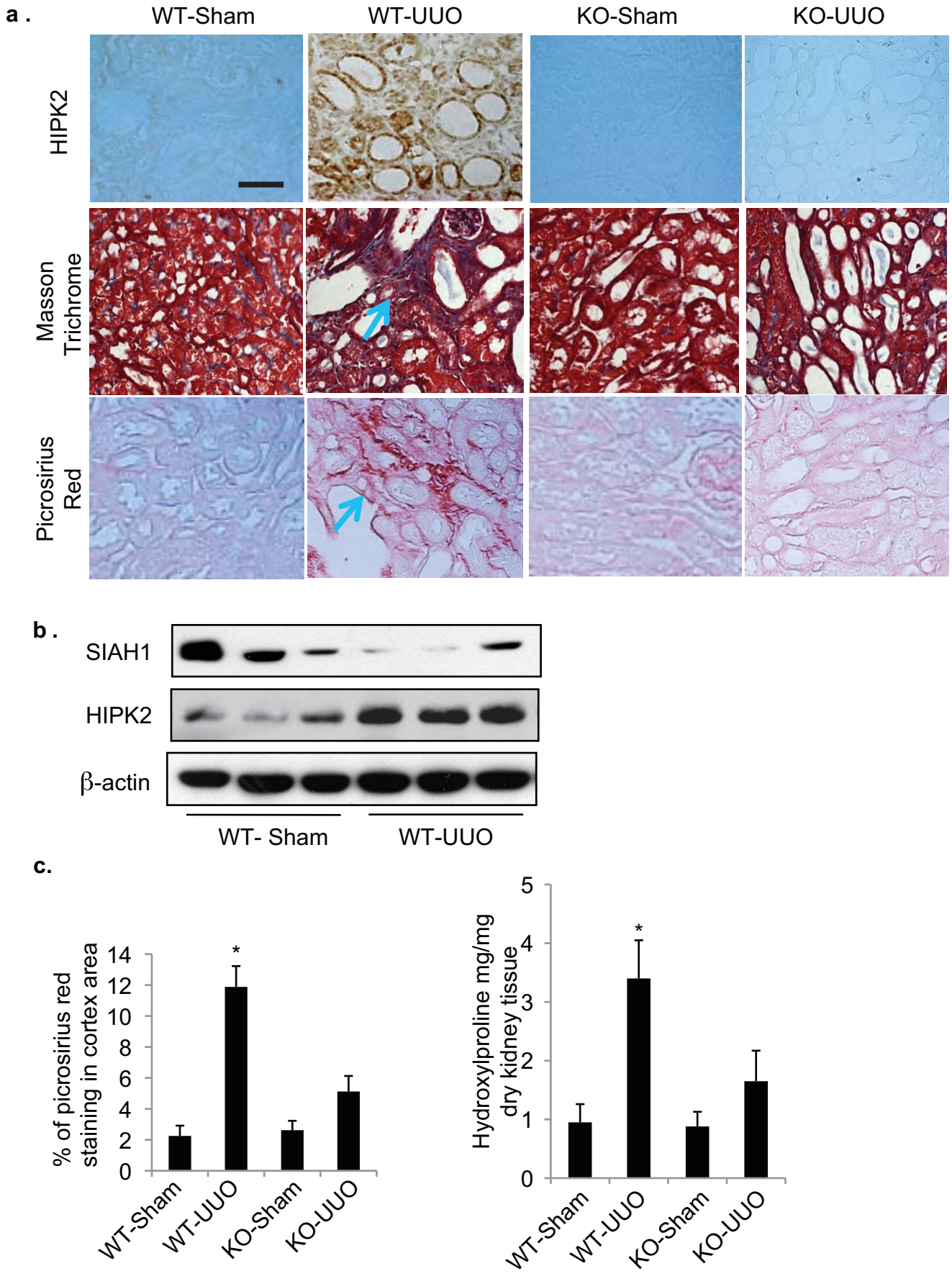

Supplementary Figure 5d-e

d.

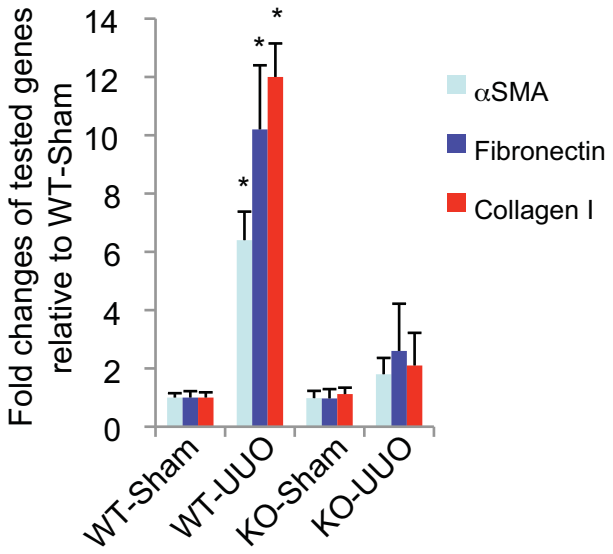

e.

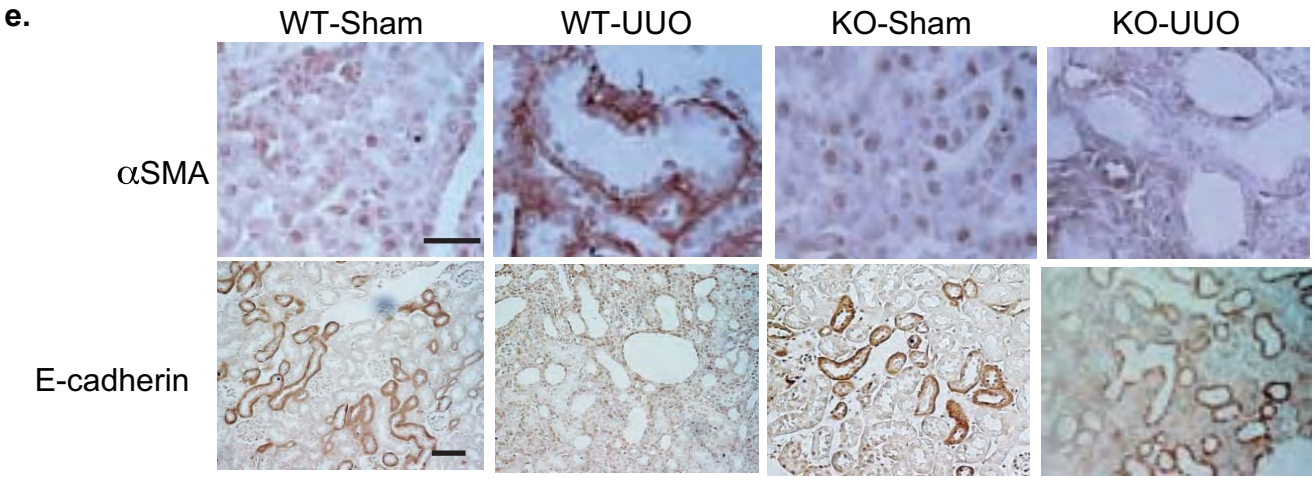

Supplementary Figure 5f-h

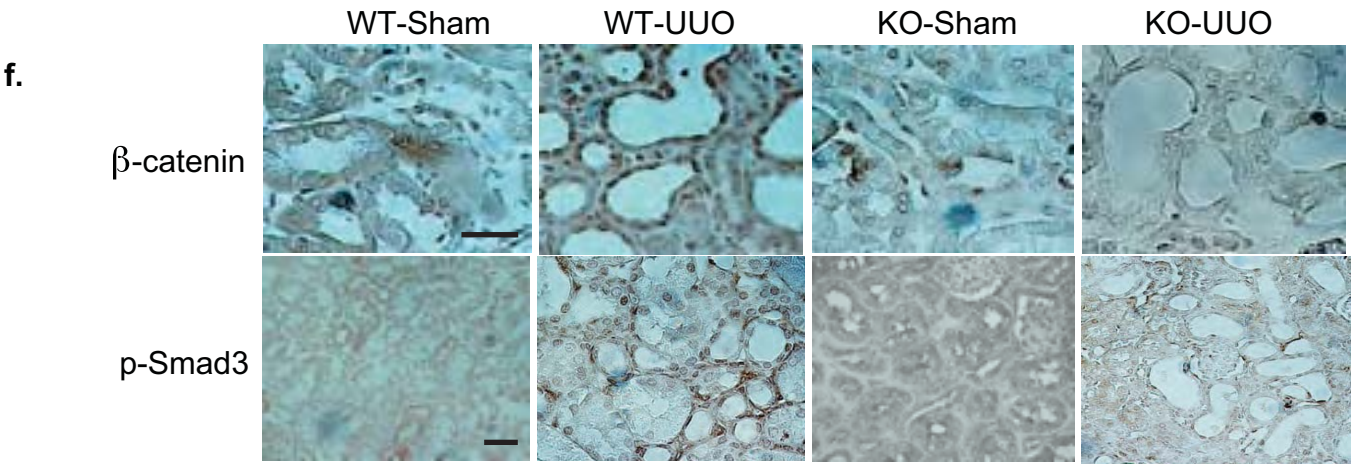

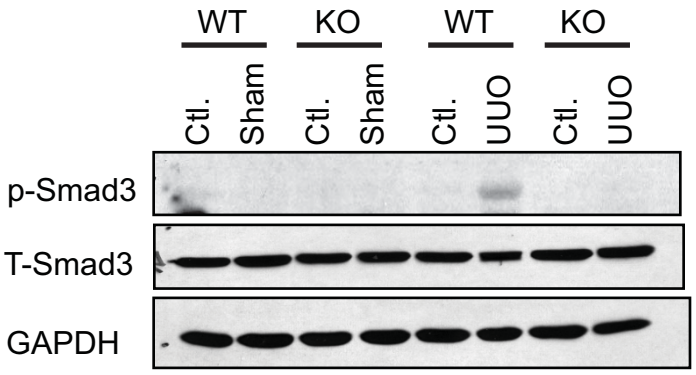

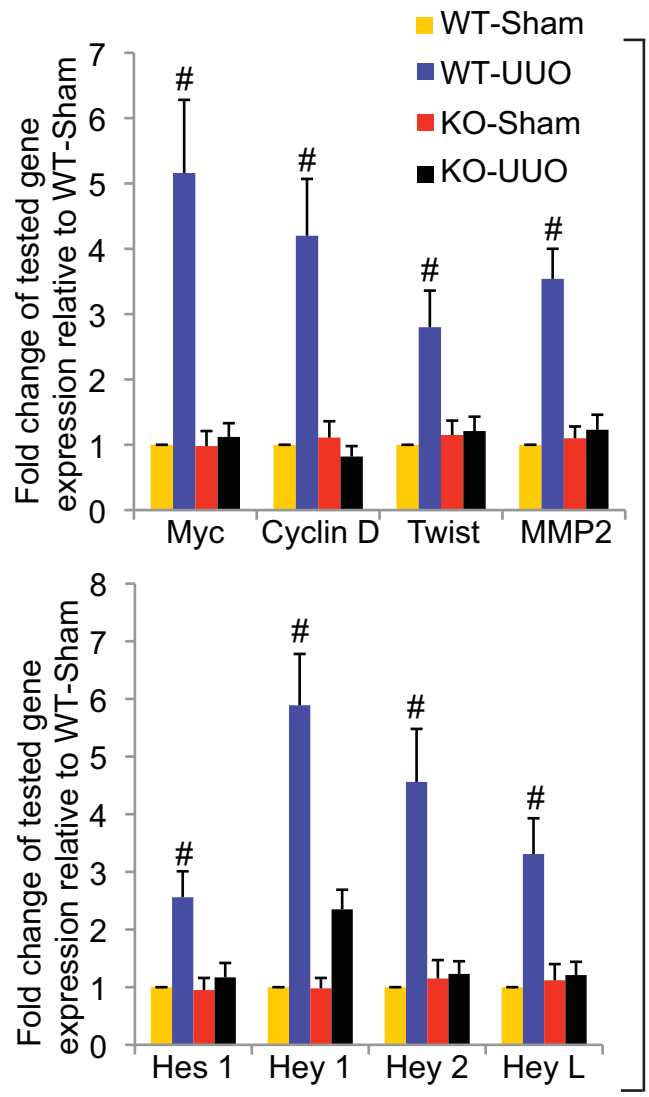

Supplementary Figure 5: HIPK2 knockout mice are protected from renal fibrosis in the unilateral ureteral obstruction (UUO) model. HIPK2 immunostaining (**a. top panel**) and Masson Trichrome (**a. middle panel**) and picrosirius red staining (**a. bottom panel**) of kidney sections from wild-type (WT) and HIPK2 knockout (KO) mice 7 days after UUO or sham procedure. Arrows indicate fibrotic area. (**b**) Western blots of SIAH1, HIPK2 and β-actin using protein lysates from the kidney cortex. Amount of renal fibrosis was determined by morphometric analysis of picrosirius red staining (**c. left panel**) and measurement of tissue hydroxylproline content (**c. right panel**). Expression of epithelial mesenchymal transition markers in kidney sections was assessed by real time PCR (**d**) and immunohistochemistry (**e**). (**f. top panel**) Activation of β-catenin was confirmed by immunostaining. Activation Smad3 signaling was confirmed by phospho-Smad3 (p-Smad3) immunohistochemistry (**f. bottom panel**) and western blots (**g**) of p-Smad3 and total Smad3 (T-Smad3) from nuclear lysates of sham-operated or UUO kidney compared to the contralateral (Ctl) kidney. Expression of Wnt-β-catenin target genes (**h. upper panel)** and Notch pathway (**h. lower panel** target genes were quantified by real time PCR. *$p<0.01$ compared to KO-UUO mice. #$p<0.01$ compared to KO-UUO, n=5 for all groups. Scale bar, 50μm.

Supplementary Figure 6a-d

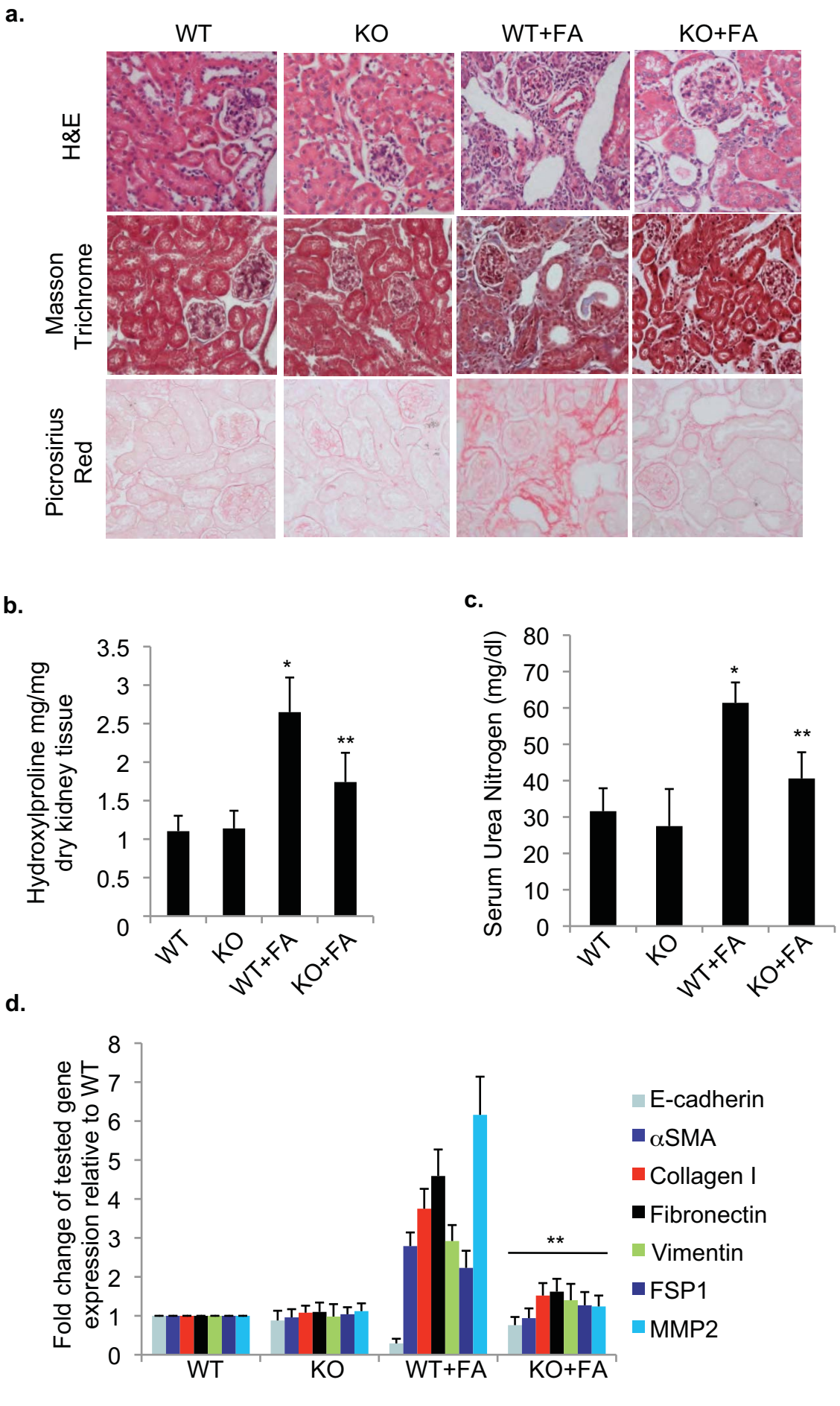

Supplementary Figure 6: HIPK2 knockout mice are protected from renal fibrosis induced by folic acid. (**a**) Kidney sections of HIPK2 wild type (WT) and knockdout (KO) mice with and without folic acid (FA)-induced kidney injury stained with hematoxylin and eosin (H&E), Masson Trichrome, and picrosirius red staining. Kidney hydroxoylproline content (**b**), serum urea nitrogen concentration (**c**), and renal expression of epithelial mesenchymal transition markers (**d**) for the four experimental groups. *$p<0.01$ compared to WT. **$p<0.05$ compared to WT+FA, n=10 for each group.

Supplement Table a: Summary of histologic scoring for kidney sections of Tg26 and WT mice.

	Kidney Histology				
	Glomerular Collapse and Sclerosis	Podocyte hyperplasia (0 - 3+)	Tubular Degenerative/ Regenerative changes (0-3+)	% Cortex with Casts / Cysts	% Tubular atrophy/ Interstitial Fibrosis
All WT (n=7)	0%	0	0	0%	0%
Tg1	32% (18/56)	1+	0	15%	10%
Tg2	35% (13/37)	1+	1+	15%	5%
Tg3	68% (53/78)	3+	2+	15%	25%
Tg4	39% (31/80)	1+	1+	10%	10%
Tg5	49% (34/69)	2+	1+	15%	15%

Supplement Table b: Summary of protein-DNA interaction array data comparing Tg26 to WT

Upregulated	Down-regulated
AP1	TR
CBF	TR (DR-4)
Myc	Antioxidant RE
Max	AP3
NF-A3	AP4
NFE-6/CP1	GATA4
Pax1	HNF-4/COUP-TF
Pax2	L-III BP
PU1	Pax6
NFkB	PPARa
TP53	NZF-3
Stat3	WT-1
	CACC
	HF1

Supplement Table c: Summary of HIPK2 and SIAH1 staining in human kidney biopsies

		Diagnosis					
Patients (n=5)		**Normal**	**MCD**	**HIVAN**	**FSGS**	**DN**	**IgAN**
HIPK2	1	0	0	2+	1+	2+	1+
	2	0	0	3+	1+	2+	3+
	3	0	0	2+	2+	3+	2+
	4	0	1+	3+	1+	2+	1+
	5	0	0	3+	2+	1+	2+
SIAH1	1	3+	2+	0	1+	0	1+
	2	3+	3+	0	1+	0	0
	3	3+	3+	0	0	0	0
	4	3+	2+	0	1+	0	1+
	5	3+	3+	0	0	1+	0

Supplement Table d: Summary of protein-DNA interaction array data comparing HEK293 cells with and without HIPK2 over expression

Upregulated	Down-regulated
Snail	HNF-3
CEBP	OCT3 (POU5F1)
NF-kB(1)	NF-1
NF-E2	PTF1
p53(1)	Cdx-2
SIE	WT 1
SMAD/SBE	NRF1/alpha-PAL
SMAD3/4	CEBP
Stat-1	ADD-1
Stat-3	EKLF(1)
Afxh/Foxo4	ICSBP
AIC/CBF	LH2-Lim-1
Ets(1)	LyF(1)
Ets/PEA3(1)	MZFI(1)
	LF-A1

Supplement Table e: Summary of promoter analysis and WikiPathway analysis for differentially expressed genes in HEK293 with HIPK2 overexpression.

Up-regulated			
TFs from promoter analysis	**P value**	**WikiPathways**	**P value**
ATF6	0.0020234936	Hs_TGF-beta_Receptor_Signaling_Pathway_WP366_21445	0.0007867812
EP300	0.0021390061	Hs_Wnt_Signaling_Pathway_and_Pluripotency_WP399_29616	0.0044147878
SRY	0.0114170004	Hs_Wnt_Signaling_Pathway_and_Pluripotency_WP399_29197	0.0044147878
T	0.0151946386	Hs_Ovarian_Infertility_Genes_WP34_20749	0.0071376239
TFAP2B	0.0250211503	Hs_Glutathione_metabolism_WP100_20893	0.0079895619
STAT3	0.0264736979	Hs_Wnt_Signaling_Pathway_WP428_28695	0.0092597180
FOXQ1	0.0272871187	Hs_Oxidative_Stress_WP408_21540	0.0163043514
IKZF1	0.0350624489	Hs_Calcium_Regulation_in_the_Cardiac_Cell_WP536_21808	0.0169890736
RELA	0.0383015610	Hs_Fatty_Acid_Beta_Oxidation_WP143_20983	0.0213914431
HAND1	0.0392382252	Hs_G_Protein_Signaling_Pathways_WP35_20751	0.0275473791
TFAP2A	0.0453661922	Hs_Glycolysis_and_Gluconeogenesis_WP534_28564	0.0348459303
NFKB1	0.0499816987		
Down-regulated			
TFs from promoter analysis	**P value**	**WikiPathways**	**P value**
JUN	0.0092277798	Hs_Glycogen_Metabolism_WP500_21730	0.0268482131
ATF2	0.0330946247		

Supplement Table f: Summary of histologic scoring for kidney sections of Tg26 and WT mice with and without HIPK2 knockout (KO).

	Kidney Histology				
	Glomerular Collapse and Sclerosis	Podocyte hyperplasia (0 - 3+)	Tubular Degenerative/ Regenerative changes (0-3+)	% Cortex with Casts / Cysts	% Tubular atrophy/ Interstitial Fibrosis
All WT (n=4)	0%	0	0	0%	0%
Tg26	59% (45/76)	2+	2+	15%	25%
Tg26	38% (27/71)	1+	1+	15%	10%
Tg26	49% (33/67)	2+	1+	20%	20%
Tg26	39% (27/70)	1+	1+	10%	10%
All KO (n=4)	0%	0	0	0%	0%
KO-Tg26	6% (3/50)	0	0	0%	0%
KO-Tg26	0% (0/77)	0	0	0%	0%
KO-Tg26	10% (7/67)	0	0	0%	5%
KO-Tg26	5% (4/73)	0	0	0%	0%

Supplementary Methods:

Primary Renal tubular Epithelial cell (RTEC) culture: Kidney cortices from 10-week-old mice were excised, minced, and digested for 30 min at 37°C in 0.5 mg ml^{-1} collagenase (Sigma). After digestion, cortical suspensions were passed through 200 mesh followed by 325 mesh filters, then resuspended in 45% Percoll and centrifuged at 27,000g for 30 min to separate into four distinct layers. The layer enriched in proximal tubular segments was removed, centrifuged, and washed to remove the remaining Percoll, then resuspended in culture media.

Constructs and vectors: siRNA for SIAH1 (Qiagen, FlexiTube siRNA SI03037839) and HIPK2 (Thermo Scientific, Dharmacon ON-TARGET siRNA) were purchased. Negative Control (Neg Cont) siRNAs were used as negative experimental controls. Both WT and kinase-dead HIPK2 expression constructs were obtained from Dr. RH Goodman, Oregon Health and Science University, Portland[1]. Siah1 expression vector (pCMV-SPORT6 containing human *Siah1* gene) was obtained from Open Biosystems. Lentivector of HIPK2 encoding for fusion proteins of mCherry with WT-HIPK2 and KD-HIPK2 were generated by PCR subcloning of a Myc-tagged HIPK2 expression vector and a Myc-HIPK2 (K221R) mutant vector[1], respectively, using primers—5'-GCGCGAATTCGAAAGTAGAGCCAAGTTCCA-3' and 5'-CCCCGGTACCTTATATGTAAGGGTATTG-3'. PCR amplified products encode for amino acid residues 25 to 1189 of *Hipk2* (gene accession AF077659.1). PCR amplicons where subcloned into EcoRI and KpnI sites of a lentiviral expression construct (VVEW-mCherry C1; a gift from G. Luca Gusella at Mount Sinai School of Medicine, NY). Cloned lentivectors were confirmed by DNA sequencing. Over-expression of HIPK2 in RTEC was verified by real-time PCR and western blot. An empty lentivector without HIPK2 insertion was used as the control.

Transfection: Lonza Nucleofector Technology (Basic Neucleofector kit for Primary Mammalian Epithelial Cells, Program T20) was used to transfect expression constructs and siRNAs into RTEC with an efficiency of 80-90% based on GFP expression. Transfection efficiency was further verified by real-time PCR and western blot. We were able to knock down HIPK2 by 60-70% and SIAH1 by 74-82%.

Real-time PCR: Intron-spanning primer sets were designed using Primer-BLAST (NCBI) and PCR amplicons were confirmed by both melting curve analysis and agarose gel electrophoresis. Lightcycler analysis software was used for determining crossing points based on the second derivative method.

Western blot: Tissue or cells were lysed with a buffer containing 1% NP40, a protease inhibitor cocktail and phosphorylation inhibitors. For HIPK2, Smad3, p53, and p65 nuclear proteins were extracted and used. The purity of nuclear proteins was verified by western blot analysis to confirm the absence of B-Raf (cytosolic protein) and the presence of CREB (nuclear protein).

Immunostaining of cells: Cells were fixed with 4% PFA for 15 minutes and permeabilized with 0.5% Triton for 5 min at room temperature. After washing, cells were

incubated first with primary antibodies followed by fluorescently tagged secondary antibodies (anti-rabbit or anti-mouse antibodies).

Immunostaining of kidney sections: Kidney sections from mice and human kidney biopsies were prepared as described[2]. Archival human kidney biopsies were collected at Columbia University under a protocol approved by its Institutional Review Board. Biopsy samples included 5 cases of HIVAN, 5 minimal change disease (MCD), 5 idiopathic focal segmental glomerulosclerosis (FSGS), 5 diabetic nephropathy (DN), and 5 IgA nephropathy (IgAN). All these patients have GS and TIF except patients with MCD. Normal tissues from nephrectomy samples were used as the control. Immunostaining was performed using specific primary antibodies and biotinylated secondary antibodies (Vector Laboratories Inc.). Staining was revealed with avidin-peroxidase (VECTASTAIN Elite; Vector Laboratories Inc.). Slides were mounted in Aqua Poly/Mount (Polysciences Inc.) and photographed using Zeiss Axioplan 2 IE microscope with Zeiss AxioCam MRm and MRc cameras. The following antibodies to the following antigens for used: mouse and human HIPK2 (Abcam), phospho-Smad3 (Cell Signaling Technology, E-cadherin (Cell Signaling Technology), αSMA (Abcam), and β-catenin (Cell Signaling Technology) antibodies. The extent of kidney staining in human biopsies was semi-quantitatively scored on a scale of 0-4 by two independent investigators (score 0: absence of specific staining; score 1: < 25% area has specific staining for either HIPK2 or Siah1; score 2: 25 to 50%; score 3: 50-75%; score 4>75%.

NFkB reporter assay: Cells were cotransfected with the firefly luciferase reporter gene, the *Renilla* luciferase gene as an internal control, and either the KD-HIPK2 or empty expression vector. Cells were then treated with or without TNF-α for overnight. Luciferase activity was determined using a dual-luciferase assay system (Promega). The firefly luciferase activity of the NFkB reporter gene was normalized to the *Renilla* luciferase activity and expressed as fold change compared to the empty expression vector.

HIPK2 kinase activity assay: HIPK2 activity was measured in nuclear protein extracts following a protocol provided by Millipore. Recombinant HIPK2 (Millipore) was used to establish the standard curve. Myelin Basic Protein (MBP) was used as the substrate. [γ-^{33}P] ATP was diluted in a magnesium acetate buffer. HIPK2 was immunoprecipitated from cells or tissues using an anti-HIPK2 antibody (Santa-Cruz).

Mice Genotyping: Genomic DNA extracted from tail clipping was used. To detect the HIV-1 transgene (*Tg26*), we performed PCR using primers designed to amplify the HIV *nef* gene (sense 5'- GCTACCACCGCTTGAGAGAC-3', antisense 5'-GGGAGTGAATTAGCCCTTCC-3'). Since all HIV-transgenic mice are heterozygous (homozygous *Tg26* animals are not viable), a strategy to differentiate heterozygous from homozygous HIV-transgenic mice was not required. Specific primers and protocols for genotyping HIPK2 knockout (KO) mice were obtained from Dr. Eric Huang[3]. KO mice were backcrossed into FVB/N for 9 generations. Then, KO mice were crossed with Tg26 to generate HIPK2$^{+/-}$ Tg26. Finally, HIPK2$^{+/-}$ Tg26 mice were crossed each other to generate KO-Tg26, HIPK2$^{+/-}$ Tg26, and WT-Tg26 mice.

Creation of the UUO model: Male animals (n=5 per group) were anesthetized and ureteral obstruction was performed by the double ligation of the right ureter with 4-0 silk via a right flank incision. Sham-operated mice had their ureters exposed and manipulated but not ligated. Based on previous publications, we studied epithelial cell apoptosis, expression of EMT markers, and renal fibrosis at day 7 post UUO. Non-obstructed kidneys and sham-operated kidneys were used as controls. The kidneys were collected at the end of the study for histology, assessment of collagen content, western blot, and real-time PCR analysis.

Creation of the Folic acid (FA) induced acute kidney injury model: Male KO mice and their WT littermates at age of 8 weeks were used for the study, which included WT and KO mice injected with either FA or vehicle (n=10 in each group). FA was injected at 250 mg kg^{-1} or equivalent volume of vehicle by IP and then followed for 4 weeks as described [4-6]. Mice were sacrificed at age of 12 weeks.

N-acetyl-cysteine (NAC) treatment of Tg26 mice: Male Tg26 mice and their age and sex-matched control littermates were fed with NAC at 300mg/kg body weight or vehicle as described[7] by daily gavage starting at age of 4 weeks for a total of 4 weeks (n=10 mice per group). The mice were sacrificed at age of 8 weeks for collection of blood, urine, and kidneys.

Kidney histology: Kidney histology was examined after periodic acid-Schiff (PAS) staining. Histologic analyses were performed by a renal pathologist and scored for the glomerulosclerosis index, podocyte hypertrophy and hyperplasia as well as tubulointerstitial changes as described[8]. Masson Trichrome and Picrosirius Red staining were performed for assessment of collagen deposition as described[9]. The amount of cortical collagen was determined by quantify areas stained with picrosirius red[10]. Twenty non-overlapping fields at 400x magnification from each section were analyzed in a blinded manner and quantified using a digital image analysis program (MetaMorph7.6). Results are expressed as a percentage of the area of picrosirius red staining.

Affymatrix/Panomics protein/DNA arrays: The Panomics protein/DNA arrays (Combo Array, Affymatrix Santa Clara CA) profiles multiple transcription factor–DNA interactions simultaneously. Nuclear proteins were extracted following manufacturer's protocol. For quantitative analysis of DNA/Protein interactions, different exposure times were made to ensure that only films with control spots that have approximately equal signal intensities were used for subsequent analyses. Densitometric analyses of scanned films were carried out using a Dot Blot Analyzer macro for Image J (http://image.bio.methods.free.fr/dotblot.html). The mean +/- standard deviation of densitometric values was computed. Mean densitometric values for interactions that were elevated or reduced by more than 2-fold and also statistically significant ($p<0.05$) were considered to be up-regulated and down-regulated interactions, respectively.

Microarray studies: Affymatrix gene expression microarrays were performed at the Mount Sinai Institution Microarray Core Facility. The Affymatrix GeneChip® Mouse Genome 430 2.0 Array was used to profile gene expression in the kidney cortex of *Tg26* and WT mice. Affiymatrix Human Gene 1.0 ST Array was used to profile gene expression in HEK293 with or without HIPK2 overexpression. One-way analysis of

variance test (ANOVA) was applied to the dataset to identify the genes that were differentially expressed between the two groups. P-values were corrected using Benjamini–Hochberg false discovery rate (FDR) with a threshold of 0.05.

Quantitative determination of tissue hydroxyproline: Kidney samples were dried at 110^{o}C for 48hrs and then accurately weighted. Dry kidneys were hydrolyzed in sealed, oxygen-purged glass ampoules containing 2ml of 6N HCL at 110^{o}C for 24 hrs. Hydroxyproline content in the hydrolysates was chemically quantified according to the techniques previously described[11]. Tissue hydroxyproline content was expressed as mg mg^{-1} dry kidney weight.

Measurement of GSH/GSSG ratio: Reduced glutathione (GSH) and oxidized gluthathione (GSSG) were analyzed in tissue lysates of kidney cortices with a colorimetric reaction kit (OxisResearch; Portland, OR) using a modified protocol as previously described[12]. The GSH and GSSG levels were first normalized to the protein concentration of kidney tissue lysates and the ratio of GSH to GSSG was determined.

Isolation of glomeruli from mice for western blot and real-time PCR: Mouse glomeruli were isolated as described[13,14]. The purity of glomerular was verified under microscopy and by western blot analysis for podocyte specific markers including synaptopodin, nephrin, and WT-1.

Statistical analysis: Data were expressed as mean±standard deviation (X±SD). The unpaired T-test will be used to analyze data between 2 groups after determination of data distribution. The Bonferroni correction was used when more than two groups were present. Statistical significance will be considered when $p<0.05$.

Computational network analysis: Promoter analysis was conducted by utilizing the TRANSFAC binding matrices processed files downloaded from the UCSD Genome Browser (hg18, tfbsConsSites). Data from this file was converted into a GMT file as defined by MSigDB (Broad Institute, MIT). Enrichment for binding sites was assessed using the Fisher exact test with p-value 0.01 threshold with the Bonferroni's correction. ChIP enrichment analysis was applied using ChEA. Protein interaction subnetworks were created using the shortest path algorithm that connects pairs of seed nodes with one intermediate step. The protein interactions databases HPRD, BioGRID, MINT, IntAct, PPID, and DIP were used to connect seed transcription factors. Kinase enrichment analysis was conducted using KEA which utilized the Fisher exact test and a database of kinase-substrate interactions we created from Phosphosite, Phospho.ELM, NetworKIN, HPRD and PhosphoPoint to rank kinases given an input list of substrates.

References:

1. Zhang, Q., Yoshimatsu, Y., Hildebrand, J., Frisch, S.M. & Goodman, R.H. Homeodomain interacting protein kinase 2 promotes apoptosis by downregulating the transcriptional corepressor CtBP. *Cell* **115**, 177-186 (2003).
2. He, J.C.*, et al.* Nef stimulates proliferation of glomerular podocytes through activation of Src-dependent Stat3 and MAPK1,2 pathways. *J Clin Invest* **114**, 643-651 (2004).
3. Winter, M.*, et al.* Control of HIPK2 stability by ubiquitin ligase Siah-1 and checkpoint kinases ATM and ATR. *Nat Cell Biol* **10**, 812-824 (2008).
4. Long, D.A.*, et al.* Angiopoietin-1 therapy enhances fibrosis and inflammation following folic acid-induced acute renal injury. *Kidney Int* **74**, 300-309 (2008).
5. Doi, K.*, et al.* Attenuation of folic acid-induced renal inflammatory injury in platelet-activating factor receptor-deficient mice. *Am J Pathol* **168**, 1413-1424 (2006).
6. Bielesz, B.*, et al.* Epithelial Notch signaling regulates interstitial fibrosis development in the kidneys of mice and humans. *J Clin Invest* **120**, 4040-4054.
7. Ivanovski, O.*, et al.* The antioxidant N-acetylcysteine prevents accelerated atherosclerosis in uremic apolipoprotein E knockout mice. *Kidney Int* **67**, 2288-2294 (2005).
8. D'Agati, V. Pathologic classification of focal segmental glomerulosclerosis. *Semin Nephrol* **23**, 117-134 (2003).
9. He, W.*, et al.* Wnt/beta-catenin signaling promotes renal interstitial fibrosis. *J Am Soc Nephrol* **20**, 765-776 (2009).
10. Junqueira, L.C., Bignolas, G. & Brentani, R.R. Picrosirius staining plus polarization microscopy, a specific method for collagen detection in tissue sections. *Histochem J* **11**, 447-455 (1979).
11. Yang, J., Dai, C. & Liu, Y. Hepatocyte growth factor gene therapy and angiotensin II blockade synergistically attenuate renal interstitial fibrosis in mice. *J Am Soc Nephrol* **13**, 2464-2477 (2002).
12. Cai, W.*, et al.* Reduced oxidant stress and extended lifespan in mice exposed to a low glycotoxin diet: association with increased AGER1 expression. *Am J Pathol* **170**, 1893-1902 (2007).
13. Takemoto, M.*, et al.* A new method for large scale isolation of kidney glomeruli from mice. *Am J Pathol* **161**, 799-805 (2002).
14. Ratnam, K.K.*, et al.* Role of the retinoic acid receptor-alpha in HIV-associated nephropathy. *Kidney Int* **79**, 624-634.